Structures 42 (2022) 1–15

Contents lists available at ScienceDirect

Structures

journal homepage: www.elsevier.com/locate/structures

# Seismic reliability of steel SMFs with deep columns based on PBSD philosophy

J. Guadalupe Monjardin-Quevedo [a], Alfredo Reyes-Salazar [b], Dante Tolentino [c], O. Daniel Gaxiola-Camacho [b], G. Esteban Vazquez-Becerra [a], J. Ramon Gaxiola-Camacho [b,*]

[a] Department of Earth and Space Sciences, Autonomous University of Sinaloa, Mexico
[b] Department of Civil Engineering, Autonomous University of Sinaloa, Mexico
[c] Departamento de Materiales, Universidad Autónoma Metropolitana, Mexico

ARTICLE INFO

*Keywords:*
Seismic reliability
Steel special moment frames
Post-northridge connection
Structural safety
Reliability index
Performance-based seismic design

ABSTRACT

Steel special moment frames (SMFs) represent a common structural solution for buildings in earthquake-prone areas. However, when SMFs are selected by structural engineers, one of their main concerns is to satisfy the permissible drifts recommended by codes. As a common option, the use of deep columns may be a feasible alternative to reduce lateral deformation of SMFs. In this paper, the authors explore the performance of steel SMFs with deep columns by evaluating their seismic reliability. Since earthquake-resistant design is moving from the prescriptive-code to performance-based seismic design (PBSD), an alternative safety approach is integrated with the PBSD philosophy. In this way, SMFs are represented by finite elements and excited by seismic loading incorporating all major sources of nonlinearity as material behavior, geometric deformations, and connections of structural members. The novel approach is developed using the first-order reliability method, response surface method, and an advanced probabilistic scheme. The computational benefits and accuracy of the proposed method are validated using traditional Monte Carlo simulation. The implementation potential is showcased with the numerical evaluation of three 9-story steel SMFs: the first one using columns of medium size and the other two considering deep columns. The seismic reliability is extracted for every model considering serviceability performance functions correlated with performance levels of collapse prevention, life safety, and immediate occupancy. In addition, the contribution of the post-Northridge connection in the steel SMFs is incorporated. Finally, without being too much critical, the use of deep columns in the models of this paper seems to be a step in the right direction to reduce weight, decrease cost, and increase structural reliability. However, it must be stated that deep columns considered in the models have no instability concern because of their low slenderness ratios.

## 1. Introduction

Seismic force-resisting systems in buildings are designed to resist the lateral demand provoked by earthquakes. One of the most popular of them are steel special moment frames, hereafter referred as simply SMFs. The main advantage of SMFs as a lateral force-resisting system is the absence of diagonal braces and/or structural walls as part of their elements, which may be very attractive to architects and owners, since free view lines can be available in open bays [23]. On the other hand, steel SMFs are generally more costly to construct than other type of seismic force-resisting systems because they involve the use of heavier steel sections and special labor for beam-to-column connections [23]. However, since SMFs transmit smaller forces to the foundation, in comparison with other lateral force-resisting systems, more economical foundation systems are required. In terms of structural design of SMFs, the selection of the size of the members is based on three main goals: (1) to control drifts below allowable values, (2) to avoid P-delta instabilities, and (3) to meet the terms of the strong-column weak-beam criteria [2]. Since the late nineties, many structural engineers have been implementing deep sections for columns in steel SMFs (W24, W27, and larger shapes) to control drifts, meet the strong-column weak-beam criteria, and satisfy post-Northridge earthquake requirements. At the same time, as a result of several investigations on the structural performance of steel SMFs in the aftermath of the 1994 Northridge

* Corresponding author.
*E-mail addresses:* jesus.monjardinq@uas.edu.mx (J.G. Monjardin-Quevedo), reyes@uas.edu.mx (A. Reyes-Salazar), dantetl@azc.uam.mx (D. Tolentino), oscargaxiola@uas.edu.mx (O.D. Gaxiola-Camacho), gvazquez@uas.edu.mx (G.E. Vazquez-Becerra), jrgaxiola@uas.edu.mx (J.R. Gaxiola-Camacho).

https://doi.org/10.1016/j.istruc.2022.06.001
Received 30 September 2021; Received in revised form 1 June 2022; Accepted 1 June 2022

earthquake [10–16], an important number of researchers started the development of studies on the seismic behavior of steel SMFs with deep columns, since the majority of the above-mentioned studies were conducted using shallow wide-flange column sections (e.g., W14 shapes).

By the beginning of the 2000 s, Chi & Uang [7] studied the cyclic behavior of deep wide-flange column sections and developed procedures and recommendations for their seismic design. Such a study was focused on the seismic performance of deep column sections when a reduced beam section moment connection is implemented. This connection became very popular after the 1994 Northridge earthquake because of its capability of moving out the plastic hinge formation from the beam-to-column flange groove welds. Based on the results documented in the above-mentioned research, when deep columns sections are used in steel SMFs, extra lateral bracing near the beam-to-column connection may be necessary to decrease lateral-torsional buckling amplitude. However, in the experimental work, only three columns were tested, and the axial load effect was completely ignored. Additionally, just one loading history was applied to the specimens. In the same year, Shen et al. [33] published a technical report where several issues related to the use of deep columns in steel SMFs were addressed. In brief, they did not report any reason to prevent the use of deep column sections in steel SMFs. However, only one ground motion was used to excite the structures under consideration, creating a necessity to explore the seismic performance of steel SMFs considering different earthquake excitations. Two years later, Sabol [32] indicated that member strength normally does not govern the design of SMFs, what really does is the drift requirement. In this way, it was justified the use of deep columns in steel SMFs. Another contribution to the use of deep columns was reported by Zhang & Ricles [38]. In such research, they demonstrated that it was unfounded the vulnerability of steel SMFs with deep columns mainly because composite floor slab provides sufficient restraint. Although six specimens were considered, the contribution of axial load in columns was assumed to be minimal and somehow neglected. Hence, based on the previously discussed research and the evolving use of deep sections in steel SMFs, in 2011, a research plan to study the seismic performance and propose design methods for deep steel beam-column members was published [25]. Parallel to such a research program, some other scholars continued investigating the seismic performance of steel SMFs with deep columns. For example, Sophianopoulos & Deri [35] overviewed the possible implementation of them in the European Standards. They concluded that the use of steel SMFs with deep columns, particularly considering reduced beam section moment connections, is underestimated in Europe [35]. Furthermore, in 2014, a study was documented where response history analyses were developed for steel SMFs considering deep columns. In this research, the seismic behavior of steel SMFs was investigated, reaching the conclusion that drifts are reduced when deep column sections are implemented [30]. However, neither the contribution of the beam-to-column connection nor the full range of instabilities that may occur in steel SMFs with deep columns was considered.

In a major advance, an increasing number of studies on the cyclic performance of deep wide-flange shapes, used as columns in steel SMFs, through experimental and finite element analysis have been reported [8,17,9]. The main findings of such investigations are the following: (1) results from finite element analyses suggested that modeling recommendation for predicting pre-capping rotation is overestimated for steel shapes with high web [8], (2) a main issue influencing the behavior of deep columns is the global out-of-plane slenderness [17], (3) the effective buckling length of deep columns may be considerably superior than its primary value [17], and (4) out-of-plane deformations are amplified by bidirectional loading but the overall performance of deep columns is not affected [9]. Recent evidence on the seismic collapse response and highly ductile limits of steel SMFs with deep columns was documented by Wu *et al.* [36,37]. In such investigations, a set of deep columns including a wide range of both local and global slenderness ratios was studied to investigate and codify the effects of different web slenderness levels, global slenderness, and axial loading [36]. In addition, the collapse potential of steel SMFs was reported in terms of column section properties, level of column gravity load, and column lateral bracing [37]. Based on the findings, design-oriented expressions were proposed for highly ductile deep columns, and it was demonstrated that the performance of steel SMFs can be better if the axial load levels on exterior columns are controlled [36,37]. Therefore, the study of the seismic performance of deep columns in steel SMFs is clearly a worldwide topic. Recently, the seismic behavior of deep columns employing European sections was investigated, making particular emphasis on the design of reduced web section connections [5]. In the same direction, the latest technological advances have demonstrated the importance of numerical and experimental studies of full-scale steel columns in steel SMFs, including deep shapes, under complex seismic loading [6]. Moreover, latest research demonstrated the importance of ductility demands of low-, mid- and high-rise steel buildings with medium and deep columns [28]. Finally, recent studies documented by other scholars demonstrated that deep, slender columns may experience important flexural strength degradation because of plastic hinge formation. The observations were validated by full-scale testing and numerical simulations. At the end, limits on slenderness ratios were proposed to limit the severity of strength degradation and axial shortening in steel SMFs with deep columns [27].

Despite decades of research on the seismic performance of deep columns in steel SMFs, several questions regarding their seismic reliability and/or vulnerability remain to be addressed. In general, the existing studies are based on deterministic analyses only. In this manner, there is a necessity to move forward to the probabilistic examination of steel SMFs with deep columns. Thus, uncertainties related to load and resistance parameters must be incorporated in the process of safety evaluation. Moreover, to extract as accurate as possible their seismic performance, several nonlinear response history analyses must be considered in the reliability assessment. Alternatively, seismic design is moving from the prescriptive-code approach to the performance-based seismic design (PBSD) philosophy [20]. Consequently, the incorporation of PBSD philosophy in the calculation of structural reliability is a correct step forward into the resilient design of steel SMFs with deep columns. Hence, several issues regarding the seismic performance of SMFs with deep columns need to be addressed.

In summary, the main objective and contribution of this paper is to extract the seismic reliability of steel SMFs with deep columns with the help of a novel reliability approach based on the first order reliability method (FORM), response surface method (RSM), and an advanced probabilistic scheme; something unique and novel for risk evaluation of structures. Uncertainty of both load and resistance parameters is properly integrated in the technical procedure as well as the PBSD philosophy. Numerical validation of the proposed method is showcased with the help of a 2-story steel SMF which is subjected to three different ground motions recorded during the 1994 Northridge earthquake. Results are compared with traditional Monte Carlo Simulation (MCS). Once the novel reliability approach is validated, its implementation is demonstrated by extracting the seismic risk of three 9-story steel SMFs: two of them with deep columns and the other one using shallow shapes. Serviceability limit states are evaluated for overall and inter-story drifts, respectively, considering collapse prevention (CP), life safety (LS), and immediate occupancy (IO) performance levels. In addition, the contribution of post-Northridge beam-to-column connection is considered in the safety evaluation of the steel SMFs.

## 2. Performance-based seismic design philosophy

During the last two decades, PBSD philosophy has been evolving and becoming popular among structural engineers. However, there are still several shortcomings in this philosophy, particularly related to the achievement of precise definitions of performance objectives, the calculation of performance levels, and the extraction of structural reliability using nonlinear response history analyses. According to the literature, the use of PBSD for design and/or assessment of structures has led to fast developments to improve the attractiveness of this philosophy [22]. Technically speaking, the main goal of the PBSD philosophy is to design a structure that will perform well when excited by different ground motions, satisfying proper performance levels associated to such earthquake excitations. In this sense, the two principal objectives of the PBSD philosophy are the following: (1) to guarantee that hazards are treated consistently by linking structural requirements with performance expectations, and (2) to assure that the losses are associated with damages of the inferred performance expectations. In addition, it has been documented that one of the major challenges of the PBSD philosophy is the lack of computational tools to extract seismic reliability of structures [20]. For a better understanding of the process behind the PBSD philosophy, Fig. 1 is introduced.

Based on what is presented in Fig. 1, the process of the PBSD philosophy may be described as follows. First, there must be a consensus on the selection of the performance objectives among decision-makers of the structure such as the owner, building official, landlord, tenants, etc. Then, the structural engineer develops a preliminary design based on the idea that it will be capable of meeting the performance objectives. At this point, the difficult part of PBSD process where the performance of the structure must be evaluated takes place. Finally, if the performance of the structure meets the performance objectives, the PBSD process comes to an end, if not, the structural design must be revised, and the structural performance of the revised design must be re-evaluated. Certainly, each step involved in the PBSD process requires a considerable amount of effort and time. In this paper, the authors propose a novel approach as an alternative to evaluate the structural performance of steel SMFs in terms of reliability information, something reported as a shortcoming in the PBSD philosophy [20].

## 3. Novel approach to extract structural reliability

Previous discussions have demonstrated the tendency of transferring seismic design from deterministic- or prescriptive-code approach to PBSD philosophy. In this way, a novel approach to extract structural risk of steel SMFs with deep columns is presented in this part of the paper as an alternative for PBSD philosophy. This approach can be used as a computational tool to evaluate the structural performance in terms of reliability index.

### 3.1. Finite element representation and analysis

A very important part of the proposed approach is the finite element (FE) representation and analysis of the structure. Thereby, considering some of its advantages over the commonly used displacement-based FE method (FEM), the Stress-Based FEM is implemented in the approach to extract deterministic seismic responses of structures [29,26,30]. The Stress-Based FEM presents several advantages, particularly for frame-

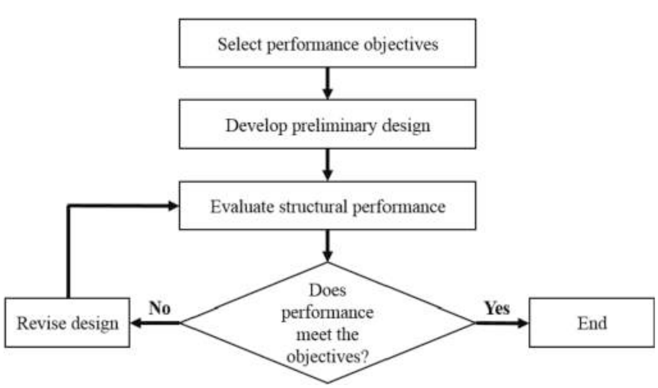


**Fig. 1.** Process of the PBSD philosophy.

type structures. A comprehensive documentation of the Stress-Based FEM is beyond the scope of this paper. However, it is widely documented in the literature where it has been extensively verified by the Authors and their research team [29,26,30,18].

### 3.2. Incorporation of Post-Northridge connection behavior

It is well-recognized that structural reliability must be extracted considering the performance of the structure as real as possible. In the aftermath of recent earthquakes, a great number of failures in numerous beam-to-column connections of steel SMFs have attracted the attention of researchers and scholars. In general, it is common that the engineering profession represents beam-to-column connections in steel structures as either simple (pinned) or rigid (fully restrained). However, the most accurate behavior of connections can be achieved by a semi-rigid connection. In other words, it is very hard to guarantee a simple (pinned) or rigid (fully restrained) connection behavior in steel structures. Thus, in very few cases, the real behavior of the connection is incorporated in the process of structural design. In theory, the structural behavior of the connection can be integrated in the structural model using its moment-rotation ($M-\theta$) curve. In this paper, the structural behavior of beam-to-column connections that were proposed right after the 1994 Northridge earthquake is included in the FEM formulation. Such joint elements, generally known as post-Northridge connections, are illustrated in Fig. 2(a).

The Post-Northridge connection presented in Fig. 2(a) is known as slotted-web steel connection [31]. This joint element was proposed to increase the ductility and improve the energy absorption during strong earthquakes. For a better understanding of the structural behavior of the slotted-web beam-to-column connections, several full-scale tests were performed following the loading protocol recommendation of the ATC-24 [4] report. The results of the tests demonstrated that when slots are implemented in the web of the beam, an appropriate structural behavior that does not compromise the initial stiffness of the connection is observed. Fig. 2(b) shows the general form of the moment-rotation ($M-\theta$) curve of the slotted-web steel connection [31]. One of the benefits of this connection is that its structural performance can be completely defined in terms of four parameters: initial stiffness ($k_i$), plastic stiffness ($k_p$), reference moment ($M_0$), and curve shape parameter ($N$). Hence, once $k_i$, $k_p$, $M_0$, and $N$ are properly obtained for a certain connection, its respective $M-\theta$ curve can be constructed. The discussion about the whole formulation of post-Northridge connections is beyond the scope of this paper, however, it is widely documented in the literature [31,19].

### 3.3. Unification of RSM and FORM

One of the most important steps of the novel approach proposed in this paper is the unification of the RSM and FORM. In this sense, to detect the failure region, an accurate response surface must be generated from the seismic performance of the structure. Such a response surface can be developed as follows. Based on the fundamental theory of RSM, the center point, sampling points, and sampling region of the response surface can be selected as [24]:

$$X_i = X_i^C + h x_i \sigma_{X_i} \text{ where } i = 1, 2, \cdots, k \qquad (1)$$

where $X_i$ is the bound or region of the $i^{th}$ random variable; $X_i^C$ represents the location of the center point corresponding to the $i^{th}$ random variable; $h$ is a subjective factor that controls the experimental sampling region; $x_i$ is the coded variable which takes values of 0, $+1$, $-1$, or $\sqrt[4]{2^k}$; $\sigma_{X_i}$ is the standard deviation of the $i^{th}$ random variable; and $k$ is the number of random variables used in the reliability analysis.

Even though Eq. (1) represents a fundamental part of RSM, such a formulation does not incorporate distributional information of random variables. Furthermore, the selection of the failure region is completely arbitrary. Therefore, the authors proposed to integrate RSM and FORM. With the help of this unification, the underlying distributional information of every random variable will be properly incorporated during every FORM iteration. However, since FORM is used in the Normal variable space, every random variable that is not Normally distributed must be transformed to an equivalent Normal random variable at the checking point. In this manner, the equivalent standard deviation ($\sigma_{X_i}^N$) and mean ($\mu_{X_i}^N$) can be extracted as follows [21]:

$$\sigma_{X_i}^N = \frac{\varnothing\{\Phi^{-1}[F_{X_i}(x_i^*)]\}}{f_{X_i}(x_i^*)} \tag{2}$$

and

$$\mu_{X_i}^N = x_i^* - \Phi^{-1}[F_{X_i}(x_i^*)]\sigma_{X_i}^N \tag{3}$$

where $\varnothing()$ and $\Phi()$ represent the probability density and cumulative distribution functions, respectively; $x_i^*$ is the checking point; and $f_{X_i}(x_i^*)$ and $F_{X_i}(x_i^*)$ are the probability density and cumulative distribution functions, respectively, of the non-normal distributed random variables at the checking point.

Finally, when all the random variables that are not Normally distributed are transformed into equivalent Normally distributed random variables, the iteration process of FORM will be started by replacing $X_i^C$ and $\sigma_{X_i}$ in Eq. (1) by $\mu_{X_i}^N$ and $\sigma_{X_i}^N$, respectively.

### 3.4. Polynomial representation of response surface

The next stage that needs to be documented in this paper is the polynomial representation of the response surface. In most of the cases, the response of structures subjected to ground motions is expected to be nonlinear. Then, the mathematical expression of the response surface must be nonlinear as well. Additionally, it is reported in the literature that if polynomials greater than second order are selected, there may be an ill-condition of the system of equations [24]. Thus, the response surface of the structure will be represented by second order polynomials without [Eq. (4)] and with [Eq. (5)] cross terms as follows [24]:

$$\widehat{p}(\boldsymbol{X}) = b_0 + \sum_{i=1}^{k} b_i X_i + \sum_{i=1}^{k} b_{ii} X_i^2 \tag{4}$$

and

$$\widehat{p}(\boldsymbol{X}) = b_0 + \sum_{i=1}^{k} b_i X_i + \sum_{i=1}^{k} b_{ii} X_i^2 + \sum_{i=1}^{k-1} \sum_{j>1}^{k} b_{ij} X_i X_j \tag{5}$$

where $b_0$, $b_i$, $b_{ii}$ and $b_{ij}$ are the unknown coefficients; $X_i$ is the $i^{th}$ random variable from $i = 1$ to $k$; and $\widehat{p}(\boldsymbol{X})$ represents the approximate response or performance function of the structural response under consideration.

Two important considerations about Eq. (4) and (5) are efficiency and accuracy of their calculation which mainly depend on the estimation of the unknown coefficients $b_0$, $b_i$, $b_{ii}$ and $b_{ij}$. For example, if one uses Eq. (4), the total number of unknown coefficients to be determined will be $2k + 1$. On the other hand, if Eq. (5) is used, a total of $(k+1)(k+2)/2$ unknown coefficients must be calculated. Consequently, if Eq. (5) is used, a more accurate polynomial representation will be obtained, but more computational efforts will be required. In addition, the definition of the most adequate polynomial representation will depend on the number of random variables ($k$). Hence, an advanced and optimal procedure must be implemented to facilitate this process.

### 3.5. Advanced probabilistic scheme to select experimental points

The selection of experimental sampling points around the center point is very important in the process to extract the structural reliability. In general, this part of the procedure defines the efficiency and accuracy that the novel approach may have. In other words, the total number of experimental sampling points represents the complete number of deterministic finite element analyses required to extract the risk of the structure. This aspect represents one of the most time-consuming parts of the approach. This is mainly why an advanced probabilistic scheme must be proposed for experimental point selection.

Two commonly used designs for selecting experimental sampling points are integrated in this paper as an advanced probabilistic scheme. They are: (1) saturated design (SD), and (2) central composite design (CCD) [24]. For the implementation of SD, either a second order polynomial without [Eq. (4)] or with cross terms [Eq. (5)] is required, and the unknown coefficients of the polynomial are generated by solving a

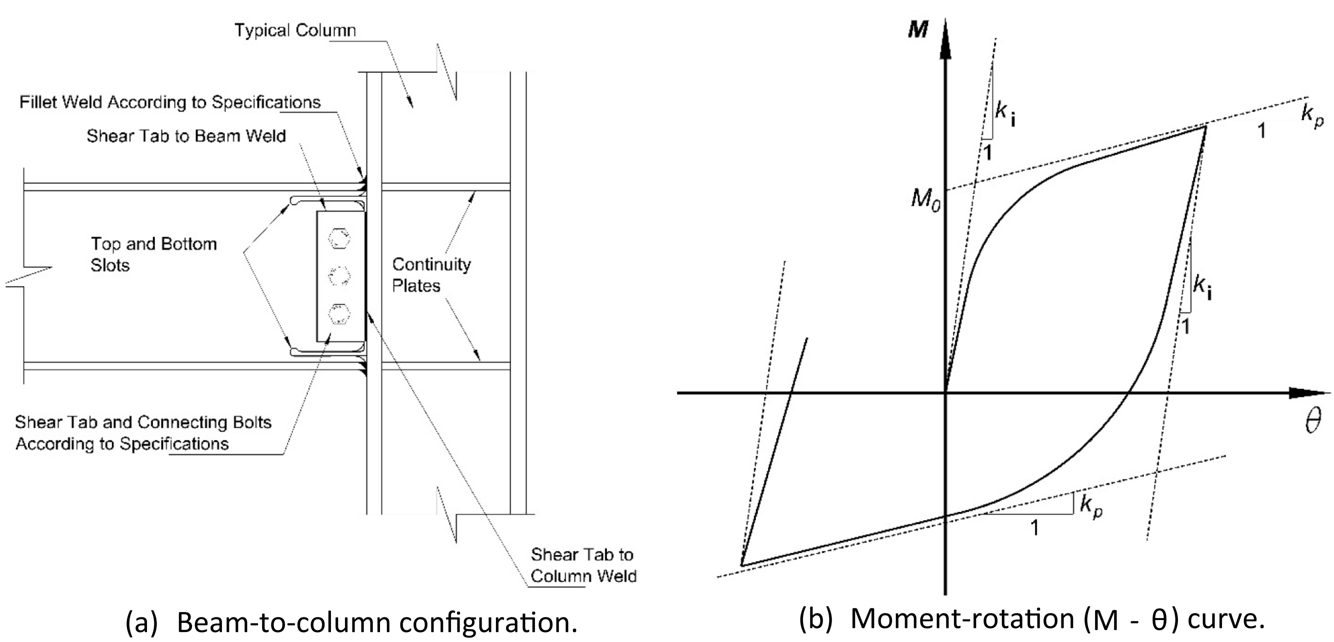


**Fig. 2.** Post-Northridge Connection.

set of equations. For the generation of a polynomial or response surface using SD, the total number of finite element analyses is equal to the total number of unknown coefficients. For example, $2k+1$ or $(k+1)(k+2)/2$ deterministic analyses will be required to construct a polynomial or response surface using SD with a polynomial without and with cross terms, respectively. In contrast, for the application of CCD, a second order polynomial with cross terms is necessary, as the one documented in Eq. (5), and regression analysis will be required to extract the unknown coefficients. The total number of deterministic analyses required to construct a polynomial with cross terms or response surface using CCD is equal to $2^k + 2k + 1$. Hence, to estimate the reliability of a structure considering 80 random variables or $k = 80$, the total number of deterministic finite element analyses required will be 161 and 3321 for SD with a polynomial without and with cross terms, respectively. Conversely, for CCD, it will require $1.20892582 \times 10^{24}$ analyses. In general, SD is more efficient than CCD. On the contrary, CCD is more accurate than SD [24]. This justifies the integration of both designs in an advanced probabilistic scheme.

During the generation of the response surface, to maintain accuracy and efficiency is the main objective of the proposed novel approach. Hence, the authors propose to reduce the number of random variables from $k$ to $k_R$; where $k_R$ is obviously the reduced number of random variables. This reduction is done by evaluating the sensitivity index of every random variable which is readily available from the FORM analysis. In this way, during the first iteration, random variables with minimal sensitivity indexes can be detected and taken as deterministic at their mean values in following iterations. For example, suppose that out of a total of 80 random variables, only 8 of them are considered very sensitive. Then, for this case, it is clear that $k_R = 8$. As a result, the total number of deterministic finite element analyses if CCD is implemented will be $2^8 + 2{*}8 + 1 = 273$. Thus, efficiency is not compromised if random variables are reduced. Based on the above, the authors propose the following probabilistic scheme to be implemented in the novel approach. During the first iteration of the method, the required response surface or performance function will be constructed using $k$ random variables and applying SD with a polynomial without cross terms [see Eq. (4)]. Then, with the help of FORM, the sensitivity index of every random variable will be extracted. Using such information, only $k_R$ number of random variables will be considered in all the following iterations. In this way, for intermediate iterations, SD and a polynomial without cross terms [see Eq. (4)] will be used again, but now considering $k_R$ random variables. Finally, for the last iteration of the novel approach, CCD and a polynomial with cross terms [see Eq. (5)] will be implemented to extract the final reliability information. For the sake of demonstrating the efficiency of the proposed advanced probabilistic scheme, imagine that the risk of a structure needs to be calculated with $k = 80$ and $k_R = 8$. Using what is proposed here and supposing that three iterations will be necessary for the risk calculation, it can be demonstrated that the number of deterministic finite element analyses will be $(2{*}k+1)+(2{*}k_R+1)+\left(2^{k_R}+2{*}k_R+1\right) = (2{*}80+1) + (2{*}8+1)+(2^8+2{*}8+1) = 451$. This is more reasonable than performing thousands or even millions of deterministic analyses that may be required when using other reliability techniques such as traditional MCS.

### 3.6. Serviceability performance levels

The next step of the approach is the generation of the required response surface in terms of the corresponding serviceability performance level. Then, if performance levels are known, the information can be used to generate the corresponding response surface. Three serviceability performance levels are defined by FEMA-350 [10] which can be used in the performance evaluation of steel SMFs: (1) immediate occupancy (IO), (2) life safety (LS), and (3) collapse prevention (CP). In addition, such serviceability performance levels are correlated to probability of exceedance, earthquake return periods, and allowable drift/ overall displacements ($\delta_{allow}$), respectively, as summarized in Table 1.

It is important to mention that the corresponding value of $\delta_{allow}$ is a function of $h$. In this sense, if overall displacement is being evaluated, $h$ will represent the total height of the steel SMF. On the other hand, if inter-story drift is being studied, the value of $h$ will be the height of the story under evaluation. Thus, the response surface in terms of a specific serviceability performance level can be expressed as:

$$p(\mathbf{X}) = \delta_{allow} - \widehat{p}(\mathbf{X}) \tag{6}$$

where $\delta_{allow}$ can be calculated from the information summarized in Table 1 for a particular serviceability performance level and $\widehat{p}(\mathbf{X})$ is the response surface obtained from the alternative approach.

### 3.7. Calculation of reliability information

The calculation of the reliability information of steel SMFs is summarized as follows. First, all the required response information will be generated at the experimental sampling points by calculating the maximum responses provoked by seismic loading using the FEs formulation. Then, during the first iteration of the novel approach, an approximation of the response surface will be generated using SD and Eq. (4). Once the first iteration is over, sensitivity indexes of every random variable will be available and a reduction of them will be performed from $k$ to $k_R$. Hence, intermediate iterations will start using $k_R$ number of random variables and another response surface will be constructed using SD and Eq. (4). Using the updated response surface, FORM will be implemented to obtain the first value of the reliability index ($\beta$). Once the first value of $\beta$ is extracted, the coordinates of the new checking point ($x_i^*$) or center point will be recalculated as:

$$x_i^* = \mu_{X_i}^N - \alpha_i \beta \sigma_{X_i}^N \tag{7}$$

where $\alpha_i$ is the value of the direction cosine which is available from every FORM iteration.

An overall updating process will continue until two consecutive values of $\beta$ converge to a pre-established tolerance level of 0.001. Hence, the final iteration will start using CCD and Eq. (5) to generate the last response surface. Once $\beta$ converges, the coordinates of the final checking point $x^*$, will be calculated as:

$$\beta = \sqrt{(x^*)^t (x^*)} \tag{8}$$

A flowchart of the alternative safety approach is illustrated in Fig. 3.

**Table 1**
Serviceability performance levels and allowable drift or overall displacements.

| Serviceability Performance Level | Probability of Exceedance | Return Period | Allowable Drift or Overall Displacement ($\delta_{allow}$) |
|---|---|---|---|
| IO | 50% in 50 years | 72-year | 0.007*$h$ |
| LS | 10% in 50 years | 475-year | 0.025*$h$ |
| CP | 2% in 50 years | 2475-year | 0.050*$h$ |

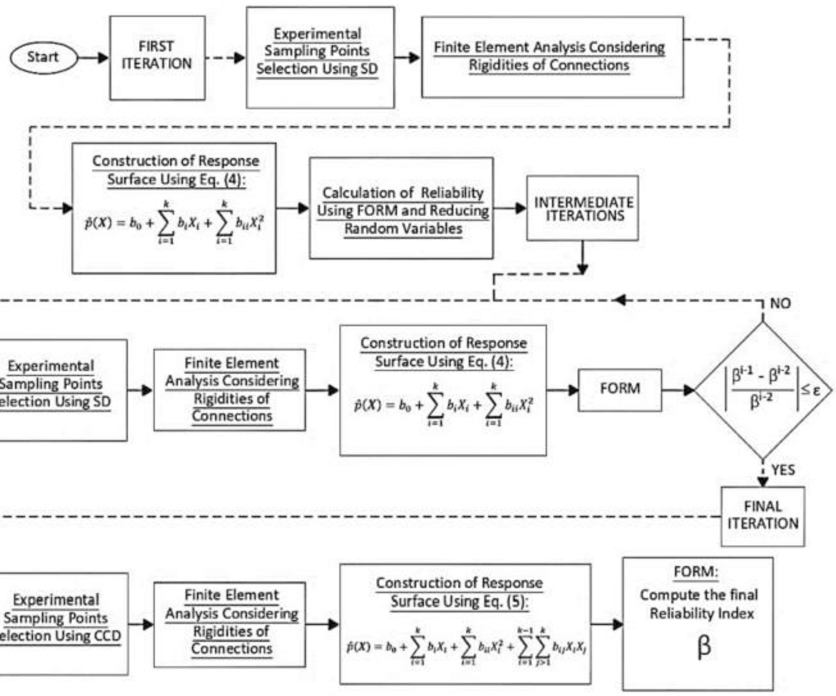


**Fig. 3.** Flowchart of the alternative safety approach.

## 4. Uncertainty in load and resistance parameters

Another important aspect to be documented is the uncertainty in load and resistance parameters that must be integrated in the process of reliability calculation of the above-mentioned novel approach. In the next section, this approach will be implemented in the risk evaluation of steel SMFs. In this way, all the structural elements under consideration will be represented by W-sections. The uncertainties related to resistance parameters are widely reported in the literature [21]. In this research, the cross-sectional area ($A$), moment of inertia ($I$), Young's modulus ($E$), yield stress of girders ($F_{yg}$) and columns ($F_{yc}$) are random variables with a Lognormal distribution with coefficient of variation (COV) of 0.05, 0.05, 0.06, 0.10, and 0.10, respectively, as shown in Table 2. In addition, the uncertainty associated with beam-to-column connections is incorporated in the process as well, considering that $k_i$, $k_p$, $M_0$, and $N$ are Normally distributed random variables with $COV$ values of 0.15, 0.15, 0.15, and 0.05, respectively. In most of the building codes around the world, structures must be designed considering dead load (DL) and live load (LL). In this study, both types of loads are represented as random variables with a Normal and Type 1 distribution, respectively, as summarized in Table 2. Furthermore, $DL_1$ and $DL_2$ represent the dead load at roof and floor levels, respectively. On the other hand, $LL_1$ and $LL_2$ are the live load for roof and floor levels, respectively. Moreover, the significance of the uncertainty in seismic loading is a challenging aspect to assess, however, it must be incorporated in the structural risk evaluation. As an alternative, the authors introduce the random variable $g_e$, representing the intensity of the ground motion under study. According to the literature, $g_e$ may follow a Type 1 distribution [21].

Finally, to incorporate the uncertainty in frequency contents of ground motions, the PBSD philosophy recommends the use of several earthquake records corresponding to specific performance levels. Thus, their corresponding probability of exceedance (PE) needs to be estimated and related to its corresponding return period. Following this

**Table 2**
Uncertainties in load and resistance parameters.

| Random Variable | Distribution | Mean Value | COV |
|---|---|---|---|
| $A(m^2)$ | Lognormal | * | 0.05 |
| $I_x(m^4)$ | Lognormal | * | 0.05 |
| $E(kN/m^2)$ | Lognormal | 1.9994E + 08 | 0.06 |
| $F_{yg}(kN/m^2)$ | Lognormal | 2.4822E + 05 | 0.10 |
| $F_{yc}(kN/m^2)$ | Lognormal | 3.4474E + 05 | 0.10 |
| $k_i(kN \bullet m/rad)$ | Normal | ** | 0.15 |
| $k_p(kN \bullet m/rad)$ | Normal | ** | 0.15 |
| $M_0(kN - m)$ | Normal | ** | 0.15 |
| $N$ | Normal | 1.0 | 0.05 |
| $DL_1(kN/m)$ | Normal | 31.8055 | 0.10 |
| $DL_2(kN/m)$ | Normal | 32.9457 | 0.10 |
| $LL_1(kN/m)$ | Type 1 | 2.9188 | 0.25 |
| $LL_2(kN/m)$ | Type 1 | 2.9188 | 0.25 |
| $g_e$ | Type 1 | 1.00 | 0.20 |

*$A$ and $I_x$ depend on the size of the member. The information can be obtained in the AISC's steel construction manual [1]. The W-shapes used for every steel SMF will be illustrated in Figs. 6–8.

**Mean values of $k_i$, $k_p$, and $M_0$ depend on the W-shape of the girder used in the beam-to-column connection. Such values can be easily obtained following the procedure documented by Gaxiola-Camacho et al. [19].

**Table 3**
Suite 1 - ground motions associated with 2% PE in 50 years and CP.

| Ground Motion | Name | SF | PGA (g) | $M_w$ | $R$(km) | Time (sec) |
|---|---|---|---|---|---|---|
| 1 | 1995 Kobe (N–S) | 1.15 | 1.282 | 6.9 | 3.4 | 25.0 |
| 2 | 1995 Kobe (E–W) | 1.15 | 0.920 | 6.9 | 3.4 | 25.0 |
| 3 | 1989 Loma Prieta (N–S) | 0.82 | 0.418 | 7.0 | 3.5 | 20.0 |
| 4 | 1989 Loma Prieta (E–W) | 0.82 | 0.473 | 7.0 | 3.5 | 20.0 |
| 5 | 1994 Northridge (N–S) | 1.29 | 0.868 | 6.7 | 7.5 | 14.0 |
| 6 | 1994 Northridge (E–W) | 1.29 | 0.943 | 6.7 | 7.5 | 14.0 |
| 7 | 1994 Northridge (N–S) | 1.61 | 0.926 | 6.7 | 6.4 | 15.0 |
| 8 | 1994 Northridge (E–W) | 1.61 | 1.329 | 6.7 | 6.4 | 15.0 |
| 9 | 1974 Tabas (N–S) | 1.08 | 0.808 | 7.4 | 1.2 | 25.0 |
| 10 | 1974 Tabas (E–W) | 1.08 | 0.991 | 7.4 | 1.2 | 25.0 |
| 11 | Elysian Park 1 (simulated) (N–S) | 1.43 | 1.295 | 7.1 | 17.5 | 18.0 |
| 12 | Elysian Park 1 (simulated) (E–W) | 1.43 | 1.186 | 7.1 | 17.5 | 18.0 |
| 13 | Elysian Park 2 (simulated) (N–S) | 0.97 | 0.782 | 7.1 | 10.7 | 18.0 |
| 14 | Elysian Park 2 (simulated) (E–W) | 0.97 | 0.680 | 7.1 | 10.7 | 18.0 |
| 15 | Elysian Park 3 (simulated) (N–S) | 1.1 | 0.991 | 7.1 | 11.2 | 18.0 |
| 16 | Elysian Park 3 (simulated) (E–W) | 1.1 | 1.100 | 7.1 | 11.2 | 18.0 |
| 17 | Palos Verdes 1 (simulated) (N–S) | 0.9 | 0.711 | 7.1 | 1.5 | 25.0 |
| 18 | Palos Verdes 1 (simulated) (E–W) | 0.9 | 0.776 | 7.1 | 1.5 | 25.0 |
| 19 | Palos Verdes 2 (simulated) (N–S) | 0.88 | 0.500 | 7.1 | 1.5 | 25.0 |
| 20 | Palos Verdes 2 (simulated) (E–W) | 0.88 | 0.625 | 7.1 | 1.5 | 25.0 |

**Table 4**
Suite 2 - ground motions associated with 10% PE in 50 years and LS.

| Ground Motion | Name | SF | PGA (g) | $M_w$ | $R$(km) | Time (sec) |
|---|---|---|---|---|---|---|
| 21 | Imperial Valley, 1940 (N–S) | 2.01 | 0.461 | 6.9 | 10 | 25.0 |
| 22 | Imperial Valley, 1940 (E–W) | 2.01 | 0.675 | 6.9 | 10 | 25.0 |
| 23 | Imperial Valley, 1979 (N–S) | 1.01 | 0.393 | 6.5 | 4.1 | 15.0 |
| 24 | Imperial Valley, 1979 (E–W) | 1.01 | 0.488 | 6.5 | 4.1 | 15.0 |
| 25 | Imperial Valley, 1979 (N–S) | 0.84 | 0.301 | 6.5 | 1.2 | 15.0 |
| 26 | Imperial Valley, 1979 (E–W) | 0.84 | 0.234 | 6.5 | 1.2 | 15.0 |
| 27 | Landers, 1992 (N–S) | 3.2 | 0.421 | 7.3 | 36 | 30.0 |
| 28 | Landers, 1992 (E–W) | 3.2 | 0.425 | 7.3 | 36 | 30.0 |
| 29 | Landers, 1992 (N–S) | 2.17 | 0.519 | 7.3 | 25 | 30.0 |
| 30 | Landers, 1992 (E–W) | 2.17 | 0.360 | 7.3 | 25 | 30.0 |
| 31 | Loma Prieta, 1989 (N–S) | 1.79 | 0.665 | 7.0 | 12.4 | 16.0 |
| 32 | Loma Prieta, 1989 (E–W) | 1.79 | 0.969 | 7.0 | 12.4 | 16.0 |
| 33 | Northridge, 1994, Newhall (N–S) | 1.03 | 0.678 | 6.7 | 6.7 | 15.0 |
| 34 | Northridge, 1994, Newhall (E–W) | 1.03 | 0.657 | 6.7 | 6.7 | 15.0 |
| 35 | Northridge, 1994, Rinaldi (N–S) | 0.79 | 0.533 | 6.7 | 7.5 | 14.0 |
| 36 | Northridge, 1994, Rinaldi (E–W) | 0.79 | 0.579 | 6.7 | 7.5 | 14.0 |
| 37 | Northridge, 1994, Sylmar (N–S) | 0.99 | 0.569 | 6.7 | 6.4 | 15.0 |
| 38 | Northridge, 1994, Sylmar (E–W) | 0.99 | 0.817 | 6.7 | 6.4 | 15.0 |
| 39 | North Palm Springs, 1986 (N–S) | 2.97 | 1.018 | 6.0 | 6.7 | 16.0 |
| 40 | North Palm Springs, 1986 (E–W) | 2.97 | 0.986 | 6.0 | 6.7 | 16.0 |

**Table 5**
Suite 3 - ground motions associated with 50% PE in 50 years and IO.

| Ground Motion | Name | SF | PGA (g) | $M_w$ | $R$(km) | Time (sec) |
|---|---|---|---|---|---|---|
| 41 | Coyote Lake, 1979 (N–S) | 2.28 | 0.589 | 5.7 | 8.8 | 12.0 |
| 42 | Coyote Lake, 1979 (E–W) | 2.28 | 0.333 | 5.7 | 8.8 | 12.0 |
| 43 | Imperial Valley, 1979 (N–S) | 0.4 | 0.143 | 6.5 | 1.2 | 15.0 |
| 44 | Imperial Valley, 1979 (E–W) | 0.4 | 0.112 | 6.5 | 1.2 | 15.0 |
| 45 | Kern, 1952 (N–S) | 2.92 | 0.144 | 7.7 | 107 | 30.0 |
| 46 | Kern, 1952 (E–W) | 2.92 | 0.159 | 7.7 | 107 | 30.0 |
| 47 | Landers, 1992 (N–S) | 2.63 | 0.337 | 7.3 | 64 | 25.0 |
| 48 | Landers, 1992 (E–W) | 2.63 | 0.307 | 7.3 | 64 | 25.0 |
| 49 | Morgan Hill, 1984 (N–S) | 2.35 | 0.318 | 6.2 | 15 | 20.0 |
| 50 | Morgan Hill, 1984 (E–W) | 2.35 | 0.546 | 6.2 | 15 | 20.0 |
| 51 | Parkfield, 1966, Cholame (N–S) | 1.81 | 0.780 | 6.1 | 3.7 | 15.0 |
| 52 | Parkfield, 1966, Cholame (E–W) | 1.81 | 0.631 | 6.1 | 3.7 | 15.0 |
| 53 | Parkfield, 1966, Cholame (N–S) | 2.92 | 0.693 | 6.1 | 8.0 | 15.0 |
| 54 | Parkfield, 1966, Cholame (E–W) | 2.92 | 0.790 | 6.1 | 8.0 | 15.0 |
| 55 | North Palm Springs, 1986 (N–S) | 2.75 | 0.517 | 6.0 | 9.6 | 20.0 |
| 56 | North Palm Springs, 1986 (E–W) | 2.75 | 0.379 | 6.0 | 9.6 | 20.0 |
| 57 | San Fernando, 1971 (N–S) | 1.3 | 0.253 | 6.5 | 1.0 | 20.0 |
| 58 | San Fernando, 1971 (E–W) | 1.3 | 0.231 | 6.5 | 1.0 | 20.0 |
| 59 | Whittier, 1987 (N–S) | 1.27 | 0.269 | 6.0 | 17 | 15.0 |
| 60 | Whittier, 1987 (E–W) | 1.27 | 0.167 | 6.0 | 17 | 15.0 |

criterion, Somerville [34] generated three suites of ground motion time histories related to 2%, 10%, and 50% PE in 50 years, respectively, for the Los Angeles (LA) area and correlated them with the performance levels of CP, LS, and IO, respectively. For each performance level, ten ground motions with two horizontal components (North-South [N-S] and East-West [E-W]) were proposed, generating twenty ground motions per suite. In summary, Somerville [34] applied scale factors (SFs) to match specific target response spectral values, on average, for several periods at 0.3, 1.0, 1.0, and 4.0 s considering a firm soil. Relevant information of such suites of ground motions is summarized in Tables 3–5 in terms of ground motion, name, SF, peak ground acceleration (PGA), magnitude ($M_w$), hypocentral distance ($R$), and time. The ground motions reported in Tables 3–5 will be used in the numerical examples of the implementation of the novel reliability approach.

## 5. Numerical Examples: Validation of the novel reliability approach and evaluation of steel SMFs with deep and shallow W-Shapes

In this section, the novel reliability approach is validated with the help of a 2-story steel SMF. Results are compared with respect to MCS. Once the approach is validated, it is implemented to extract the structural reliability of three 9-story steel SMFs: two of them using deep columns sections, and the other one considering the use of shallow W-shapes for columns.

### 5.1. Computational cost and accuracy validation of the novel reliability approach

To demonstrate the benefits in terms of computational cost and accuracy of the novel reliability approach, a 2-story steel SMF is used as a benchmark case of study. The steel SMF is subjected to three different time histories recorded during the 1994 Northridge earthquake. A small steel SMF is studied to facilitate the validation of the novel reliability approach using the well-known and traditional MCS. Fig. 4 illustrates the 2-story SMF, and the ground motions used for the validation.

In addition, fully restrained (FR) and partially restrained (PR) type of connections are considered for the study. Post-Northridge connections (see Fig. 2) with two slots in the web of the beam are used as PR connections. The required random variables to extract the reliability information of the 2-story steel SMF are summarized in Table 6. The uncertainty associated with random variables is also presented in Table 6 in terms of distribution, mean, and COV.

Furthermore, for this numerical example, the reduction in the number of random variables from $k$ to $k_R$ is performed in the next manner. Since all random variables do not have the same effect, the information on sensitivity index can be used to reduce the number of them. The sensitivity index of a random variable is its direction cosine. Because one of the methods integrating the proposed novel reliability approach is FORM, the information on direction cosines of all random variables can be readily available just after completing the first iteration of the process. Hence, for the 2-story steel SMF presented in Fig. 4, the number of random variables in the first iteration is $k = 14$. Then, for intermediate iterations, the number of random variables is reduced to $k_R = 5$. Table 7 summarizes the sensitivity indexes for the random variables when the steel frame is excited by the Canoga Park station record. In Table 7 is observed that only 5 of them are sensitive ($A_{Girders}$, $A_{Columns}$, $DL$, $LL$, and $g_e$). Based on the results of sensitivity indexes, it is expected to have highly sensitive indexes for $DL$, $LL$, and $g_e$ which are random variables related to demands acting on the structure. On the other hand, it would be expected higher sensitivity indexes for random variables related to flexure. However, $A_{Girders}$ and $A_{Columns}$ were reported

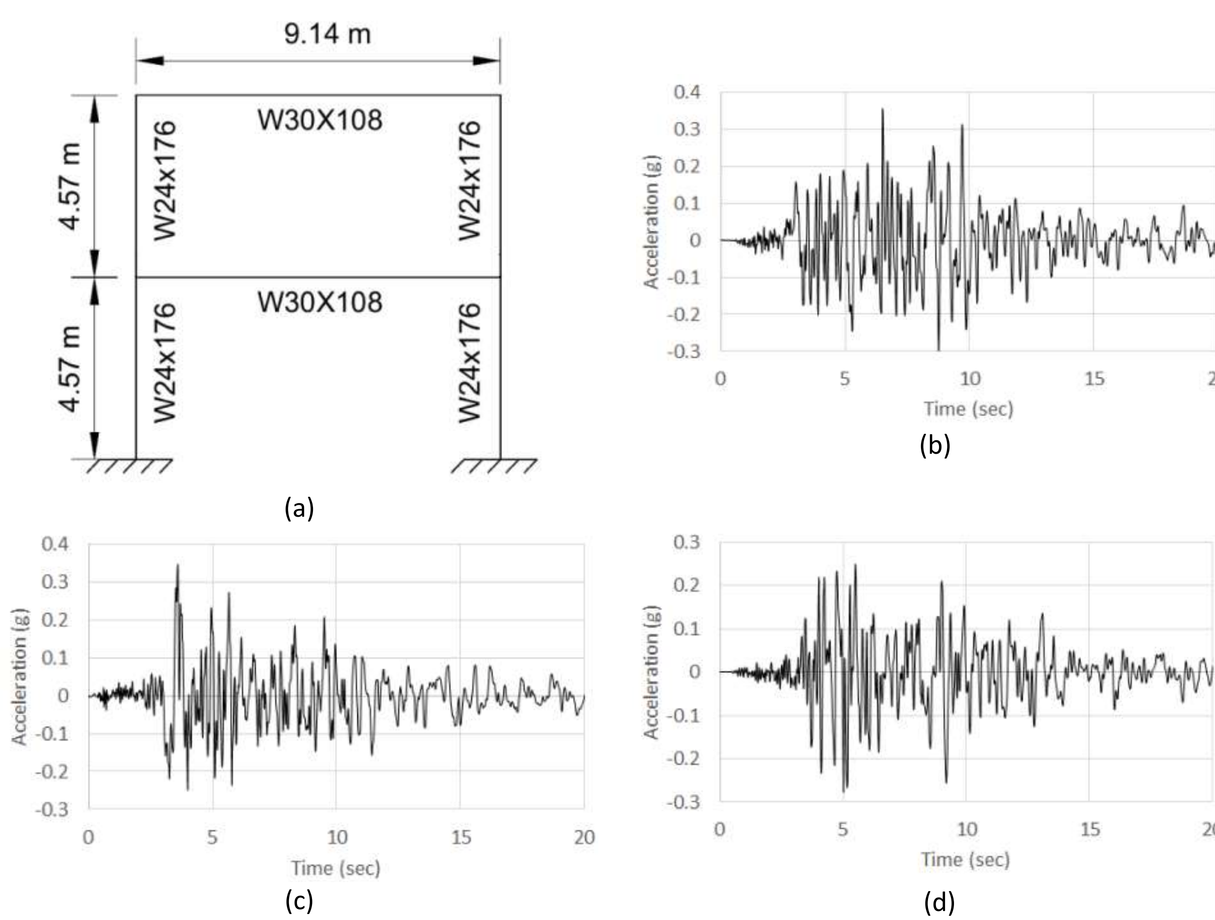


**Fig. 4.** (a) 2-story steel SMF; (b) Canoga Park station record; (c) Nordhoff fire station record; (d) Roscoe Blvd. station record.

**Table 6**
Information of random variables of the 2-Story steel SMF.

| Random Variable | Distribution | Mean ($\overline{X}$) | COV |
|---|---|---|---|
| $E$(kN/m$^2$) | Lognormal | 1.9995E + 08 | 0.06 |
| $F_{y_{Girders}}$ (kN/m$^2$) | Lognormal | 2.4822E + 05 | 0.10 |
| $F_{y_{Columns}}$ (kN/m$^2$) | Lognormal | 3.4474E + 05 | 0.10 |
| $A$(m$^2$) | Lognormal | * | 0.05 |
| $I_x$(m$^4$) | Lognormal | * | 0.05 |
| $DL$(kN/m$^2$) | Normal | 4.0219 | 0.10 |
| $LL$(kN/m$^2$) | Type 1 | 1.1970 | 0.25 |
| $k_i$(kN-m/rad) | Normal | 1.9546E+07 | 0.15 |
| $k_p$(kN-m/rad) | Normal | 4.5194E+03 | 0.15 |
| $M_o$(kN-m) | Normal | 2.0145E+03 | 0.15 |
| $N$ | Normal | 1.00 | 0.05 |
| $g_e$ | Type 1 | 1.00 | 0.20 |

*Mean values of $A$ and $I_x$ can be found in steel construction manual [1]. They are considered as random variables for every girder and column.

**Table 7**
Sensitivity Indexes for 2-Story Steel SMF Excited by Canoga Park Record.

| Number | Description | Random Variable | Sensitivity Index |
|---|---|---|---|
| 1 | Young's modulus | $E$ | 6.74114E−08 |
| 2 | Area of girders | $A_{Girders}$ | 8.31921E−01 |
| 3 | Moment of inertia of girders | $I_{x_{Girders}}$ | 5.89643E−09 |
| 4 | Yield stress of girders | $F_{y_{Girders}}$ | 5.30008E−08 |
| 5 | Area of columns | $A_{Columns}$ | 8.18823E−01 |
| 6 | Moment of inertia of columns | $I_{x_{Columns}}$ | 5.60832E−09 |
| 7 | Yield stress of columns | $F_{y_{Columns}}$ | 6.56371E−08 |
| 8 | Dead Load | $DL$ | 7.89253E−01 |
| 9 | Live Load | $LL$ | 7.20382E−01 |
| 10 | Intensity of ground motion | $g_e$ | 9.29832E−01 |
| 11 | Initial stiffness of connections | $k_i$ | 3.87426E−09 |
| 12 | Plastic stiffness of connections | $k_p$ | 8.21563E−08 |
| 13 | Reference moment of connections | $M_o$ | 7.57319E−09 |
| 14 | Curve shape parameter of connections | $N$ | 2.15973E−10 |

**Table 8**
Validation Results for 2-Story steel SMF.

| Earthquake | Performance Function | Method | FR | | PR (post-Northridge) | |
|---|---|---|---|---|---|---|
| | | | $\beta$ (NFEA) | $p_f$ | $\beta$ (NFEA) | $p_f$ |
| Canoga Park Station | Overall Drift | Alternative Reliability Approach | 3.5232 (94) | 0.000213 | 3.6208 (94) | 0.000147 |
| | | MCS | 3.5149 (50,000) | 0.000220 | 3.6331 (50,000) | 0.000140 |
| | Inter-story Drift | Alternative Reliability Approach | 3.2429 (94) | 0.000592 | 3.3357 (94) | 0.000425 |
| | | MCS | 3.2389 (50,000) | 0.000600 | 3.3139 (50,000) | 0.000460 |
| Nordhoff Fire Station | Overall Drift | Alternative Reliability Approach | 3.6949 (94) | 0.000110 | 3.8853 (94) | 0.000051 |
| | | MCS | 3.7190 (50,000) | 0.000100 | 3.8461 (50,000) | 0.000060 |
| | Inter-story Drift | Alternative Reliability Approach | 3.2954 (94) | 0.000491 | 3.5170 (94) | 0.000218 |
| | | MCS | 3.3139 (50,000) | 0.000460 | 3.5149 (50,000) | 0.000220 |
| Roscoe Blvd Station | Overall Drift | Alternative Reliability Approach | 3.6508 (94) | 0.000131 | 3.9039 (94) | 0.000040 |
| | | MCS | 3.6331 (50,000) | 0.000140 | 4.1075 (50,000) | 0.000020 |
| | Inter-story Drift | NRT | 3.2528 (94) | 0.000571 | 3.5969 (94) | 0.000161 |
| | | MCS | 3.2585 (50,000) | 0.000560 | 3.5985 (50,000) | 0.000160 |

to be more sensitive. This is justified because of the high uncertainty of seismic loading, particularly in the content of frequencies of the accelerograms. It was found as well by the authors that for Roscoe Blvd. and Nordhoff fire station earthquakes, the values of $k$ and $k_R$ for the 2-Story steel SMF are equal to 14 and 5, respectively.

Reliability index,$\beta$, and $p_f$ are extracted using the novel reliability approach for both overall lateral and inter-story drift at the second-floor level, respectively. The permissible overall lateral and inter-story drift are 2.86 and 1.43 cm, respectively. The $\beta$ and $p_f$ values for overall and inter-story drift are summarized in Table 8. They are estimated using 50,000 cycles of MCS. In other words, to extract the reliability of the 2-Story steel SMF, the number of finite element analyses (NFEA) required for the MCS were 50,000. On the other hand, using the novel reliability approach, the NFEA was limited to only 94, representing an outstanding improvement in terms of computational cost. Furthermore, in all cases, the $\beta$ and $p_f$ values obtained by the alternative reliability approach and MCS are quite similar indicating that the proposed method is accurate.

### 5.2. Steel SMFs models with shallow (W14) and deep (W27) column sections

The steel SMFs models are based on one of the buildings documented in FEMA-355C [15] report. The plan view of the building studied in this paper and the elevation of the steel SMF are illustrated in Fig. 5. It is important to mention that the steel building illustrated in Fig. 5 was designed by three consulting firms in the USA following the code specifications of the late nineties. In addition, for this research, only the exterior frame of the building which is enclosed by a rectangle in Fig. 5 (a) is used for the seismic risk analysis.

As previously mentioned, three steel SMFs are used in this paper to study the contribution of the size of the column in the seismic reliability assessment. The first model is illustrated in Fig. 6. It can be observed in Fig. 6 that only W14 sections are used for the columns of the steel SMF, which can be categorized as shallow W-shapes. Thus, based on the objectives of this paper, two other structural configurations were designed maintaining the same geometry of the steel SMF illustrated in Fig. 5(b).

In this way, a second steel SMF was designed according to a criterion based on equivalent strength which is described as follows. Plastic moments with respect to the major axis were approximately the same as those of the model of shallow W-shapes (W14). Then, deep sections were selected for the new steel SMF using W27 shapes as presented in Fig. 7. The resulting model guarantees, in certain way, an equivalence in terms of strength. It can be demonstrated that the weight of columns using W14 sections (see Fig. 6) is 60% higher than the weight of columns with W27 steel shapes (see Fig. 7). This will represent a higher cost for the steel SMF with W14 shallow shapes (see Fig. 6). The third steel SMF was designed considering equivalence in terms of weight. In other words, the

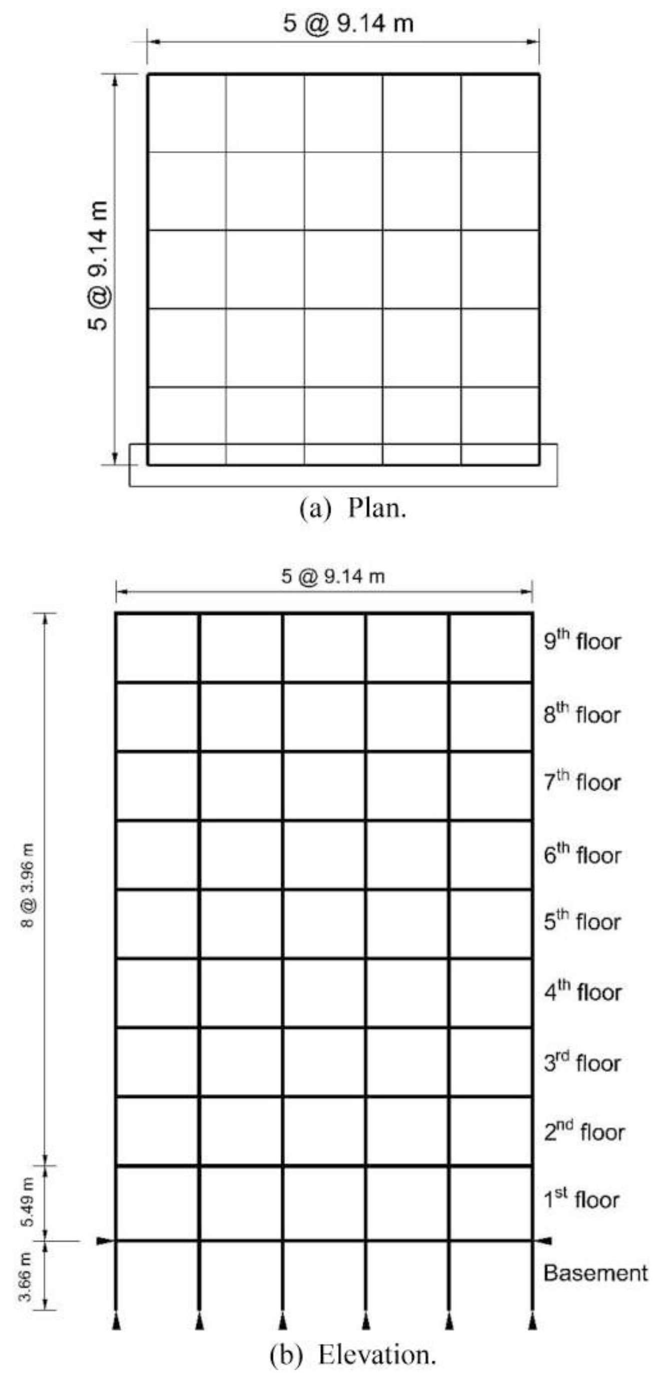


Fig. 5. Geometry of the building.

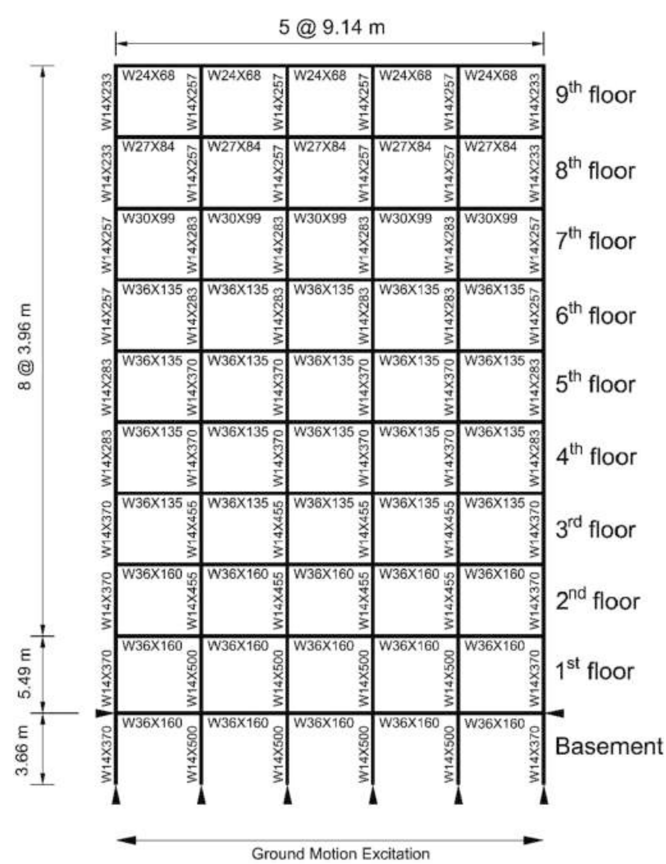


Fig. 6. Steel SMFs with W14 columns – Model 1.

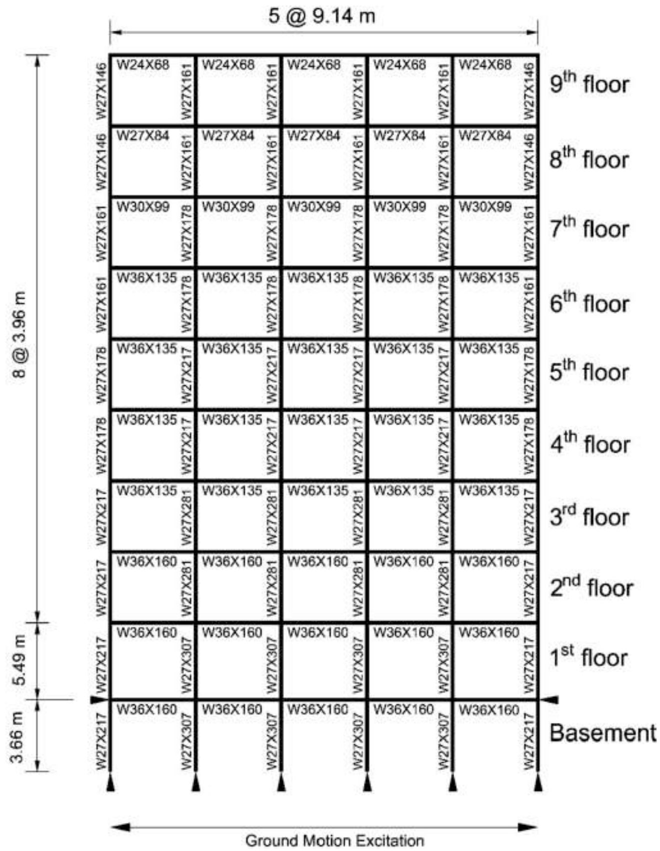


**Fig. 7.** Steel SMFs with W27 deep columns – Equivalent strength – Model 2.

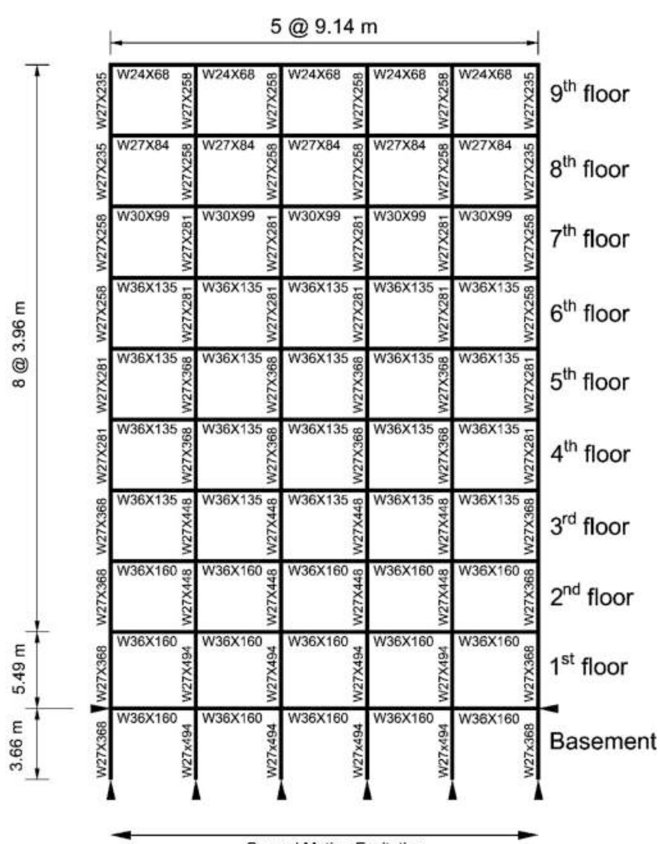


**Fig. 8.** Steel SMFs with W27 deep columns –Equivalent weight – Model 3.

structural design was obtained using deep column sections (W27) to approximately have the same weight as columns of the steel SMF with shallow W14 shapes (see Fig. 6). The steel SMF considering equivalence in weight is illustrated in Fig. 8. For the sake of discussion, hereafter the model using W14 column sections will be named Model 1, the steel SMF considering equivalence in strength will be Model 2, and the steel SMF based on equivalent weight of columns will be called Model 3.

### *5.3. Results of steel SMFs with shallow (W14) and deep (W27) column sections*

Results in this section are presented in terms of the reliability index ($\beta$) extracted by implementing the novel approach. The three steel SMFs were excited by each of the ground motions reported in Tables 3–5, to consider CP, LS, and IO performance levels, respectively. For overall drift, serviceability limits of 185.85, 92.93, and 26.02 cm were evaluated corresponding to CP, LS, and IO performance levels, respectively. On the other hand, inter-story drift was studied for the 4th floor of every steel SMF. For this case, serviceability limits of 16.8, 8.4, and 2.35 cm were utilized with respect to CP, LS, and IO performance levels, respectively. In addition, reliability indexes are calculated considering FR and PR beam-to-column connections. For the case of PR results, the structural behavior of post-Northridge connections is incorporated in the process of reliability calculation (see Fig. 2). To have a structural safety limit, the probability of collapse (PC) is incorporated. Based on what is reported in ASCE 7-16 [3], PC of structures must be at most 10% which in terms of $\beta$ is 1.25. For Model 1, 2, and 3, the total and reduced number of random variables are $k = 91$ and $k_R = 7$, respectively.

Structural reliability results of Model 1 (steel SMF with W14 columns) are illustrated in Figs. 9 and 10 corresponding to overall drift and inter-story drift, respectively. For all ground motions, it can be noted that all $\beta$ values are greater than the PC limit indicating that the structure is safe. It is important to mention that $\beta$ values considering PR connections are very similar to those of FR connections. This may be an indicator of the good performance of post-Northridge beam to column connections. For every performance level, the frequency contents of time histories played an important role in the reliability calculation. This is demonstrated by the variation of the $\beta$ values.

Figs. 11 and 12 illustrate the reliability indexes of Model 2 (steel SMF with W27 sections based on equivalent strength). Since all values of $\beta$ are greater than 1.25, it is demonstrated that Model 2 is safe for every ground motion excitation. It is observed that the reliability of the structure with PR connections is very comparable with reference to FR connections. The values of $\beta$ calculated for the two components (N-S and E-W) of the same ground motion are different. This demonstrates the fact that designing a structure for one design earthquake time history is inadequate. Thus, designing a structure using multiple time histories, as suggested in recent design guidelines [3], is correct.

The reliability results of Model 3 (steel SMF with W27 sections based on equivalent weight) are presented in Figs. 13 and 14. The results demonstrate that the risk of the structure is above the PC limit for every ground motion under consideration. Model 3, as well as Models 1 and 2, are safe for CP, LS, and IO performance levels, respectively. Variation between $\beta$ values indicate that steel SMFs respond differently depending on the frequency contents of the ground motions. Lastly, from the above results, the authors believe that permissible values suggested in design guidelines [10] are acceptable. In brief, it can be stated that $\beta$ values are within a range that satisfies the intent of the code.

Up to this point, in Figs. 9-14, the reliability indexes of the models were studied considering PR and FR beam-to-column connections for CP, LS, and IO, respectively. In addition, two serviceability limit states were evaluated: (1) overall drift, and (2) inter-story drift, respectively. To complement the discussion about the results, the authors introduce Table 9 where the mean values of the reliability index ($\beta_\mu$) are summarized with respect to serviceability limit states, performance levels, and type of connections (FR and PR). On average, in all cases, it is

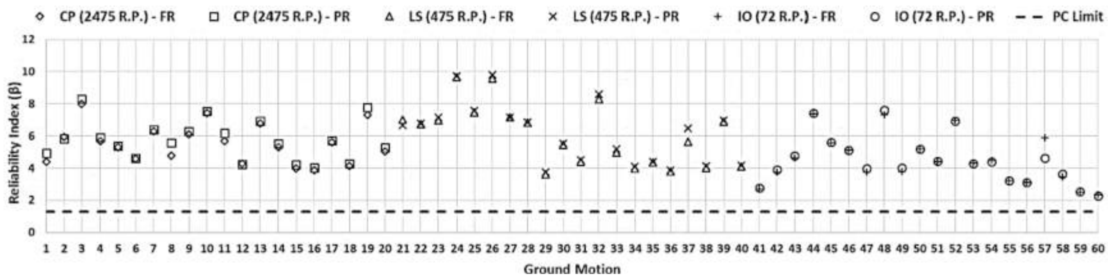


**Fig. 9.** Reliability index of overall drift – Model 1.

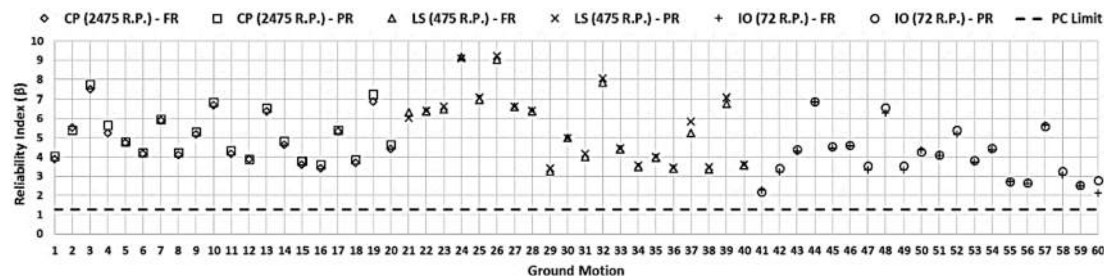


**Fig. 10.** Reliability index of inter-story drift – Model 1.

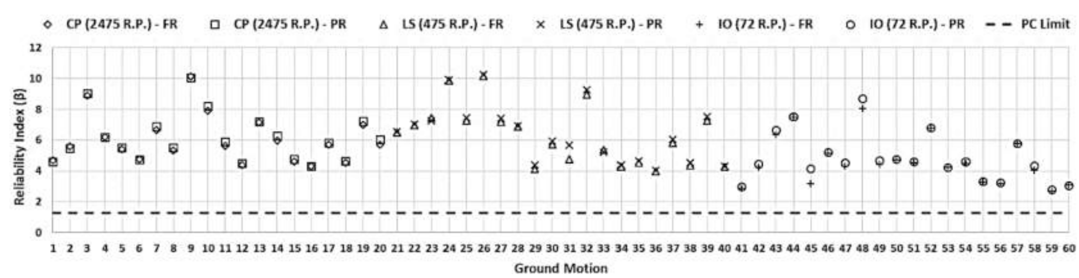


**Fig. 11.** Reliability index of overall drift – Model 2.

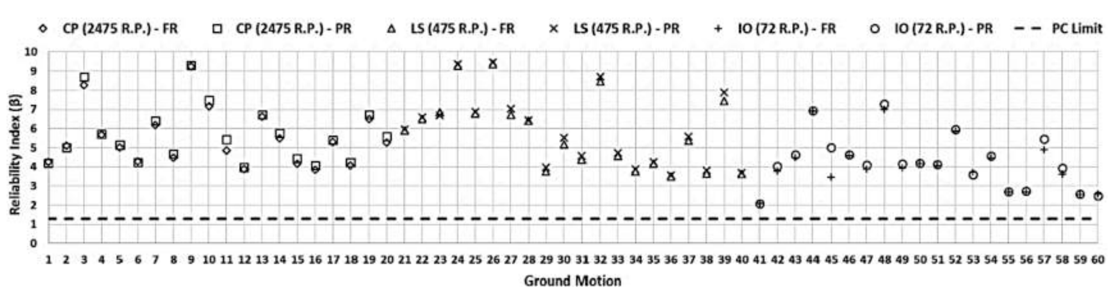


**Fig. 12.** Reliability index of inter-story drift – Model 2.

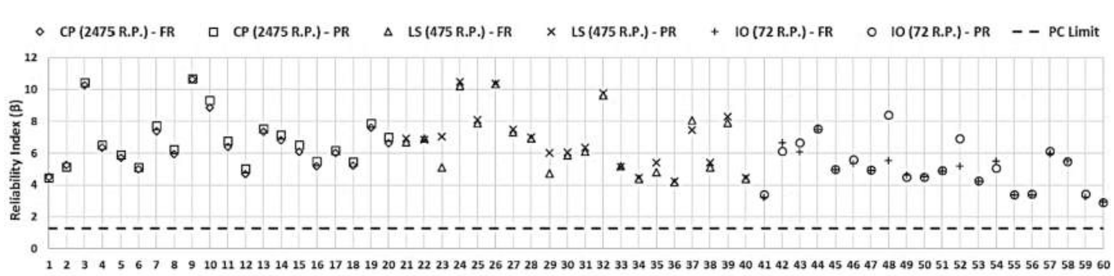


**Fig. 13.** Reliability index of overall drift – Model 3.

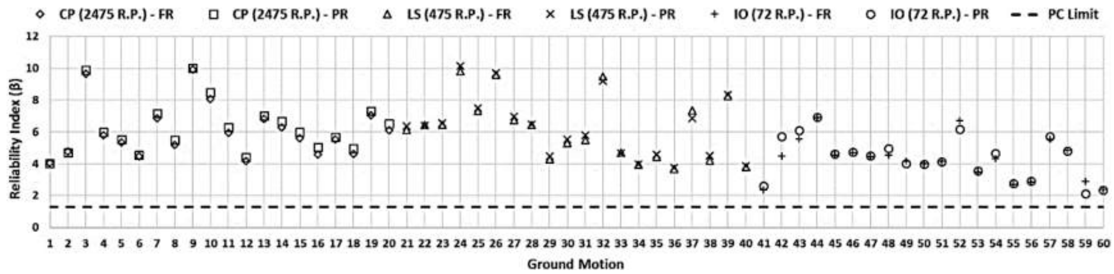


**Fig. 14.** Reliability index of inter-story drift – Model 3.

**Table 9**
Mean values of reliability index of Models 1, 2, and 3.

| Model | Performance Level | Serviceability Limit State | | | |
|---|---|---|---|---|---|
| | | Overall Drift | | Inter-story Drift | |
| | | $\beta_\mu$(FR) | $\beta_\mu$(PR) | $\beta_\mu$(FR) | $\beta_\mu$(PR) |
| 1 | CP (2% PE in 50 years) | 5.5262 | 5.7459 | 4.9718 | 5.1187 |
| | LS (10% PE in 50 years) | 6.0401 | 6.1730 | 5.5775 | 5.6823 |
| | IO (50% PE in 50 years) | 4.4941 | 4.4882 | 3.9569 | 4.0673 |
| 2 | CP (2% PE in 50 years) | 6.0233 | 6.1416 | 5.4823 | 5.6552 |
| | LS (10% PE in 50 years) | 6.2807 | 6.4339 | 5.7798 | 5.9337 |
| | IO (50% PE in 50 years) | 4.6415 | 4.8190 | 4.0694 | 4.2622 |
| 3 | CP (2% PE in 50 years) | 6.5993 | 6.8298 | 6.0444 | 6.2830 |
| | LS (10% PE in 50 years) | 6.5873 | 6.8702 | 6.1944 | 6.2851 |
| | IO (50% PE in 50 years) | 4.8784 | 5.1307 | 4.2768 | 4.3737 |

observed that inter-story drift is more critical than overall displacement, which reflects the difficulty of satisfying both serviceability limit states with the same reliability. However, although $\beta_\mu$ values for inter-story drifts are smaller with respect to the $\beta_\mu$ values of overall drift, both serviceability limit states satisfy the PC threshold of 1.25. One more important observation with reference to Table 9 is that, for all cases, Model 1 is less reliable than Model 2 and 3, and at the same time the safest of the three steel SMFs is Model 3, which is the one with deep W27 columns with approximately the same weight as the steel SMF with W14 columns. In other words, based on this observation, steel SMFs with deep columns (W27) may improve the structural reliability compared to those using shallow W-shapes (W14). The last observation with respect to Table 9 is the following. When a post-Northridge connection is used in steel SMFs, the structural reliability of the structure can be improved by the increase of its reliability index. Thus, the introduction of this connection right after the 1994 Northridge earthquake was a step in the right direction.

To demonstrate the positive contribution of the use of post-Northridge beam-to-column connections, Fig. 15 is introduced. It can be observed that, for most of the cases, reliability indexes of both serviceability limit state functions are slightly greater for the case of PR post-Northridge connections, demonstrating the improvement of structural safety.

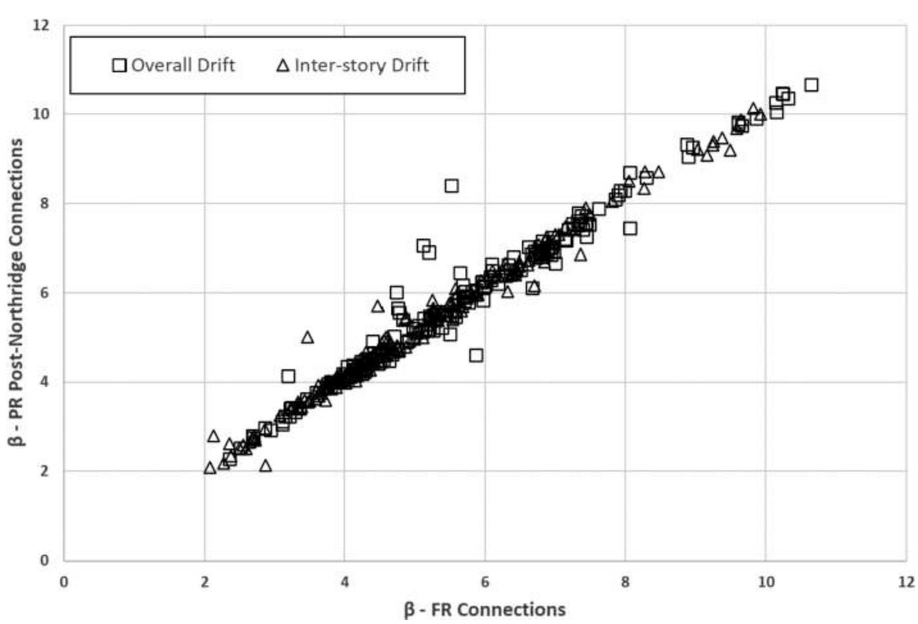


**Fig. 15.** Reliability of FR and PR Post-Northridge Connections.

## 6. Conclusions

Based on the results of this paper, the following conclusions can be documented.

A novel approach to extract structural safety of steel SMFs based on the PBSD philosophy is proposed. Such a technique can be considered as an alternative in comparison with other reliability techniques available in the literature.

The structural risk is extracted considering two serviceability limit state performance functions: (1) overall drift, and (2) inter-story drift, respectively. Based on the results, it is documented that inter-story drift is more critical than overall drift.

It is reported that the structural safety of steel SMFs can be improved if a post-Northridge connection is implemented.

The variability in the values of the reliability indexes for each of the steel SMFs clearly indicates the importance of frequency contents in the different ground motions considered in the study.

The structural safety of the steel SMFs with deep columns sections (W27) was demonstrated to be superior to the one with shallow columns (W14). Thus, the use of deep columns (W27) is a feasible option to increase the structural safety of steel SMFs.

Without compromising structural safety, the use of deep columns (W27) may provide a considerable reduction of weight and cost of steel SMFs.

For all the cases, the structural reliability was greater than the PC limit. This indicates that all the steel SMFs studied represent secure structures.

The above-documented conclusions represent a positive step forward into the efficient and accurate seismic reliability evaluation of steel SMFs with deep columns. However, since only three steel SMFs are considered in this study, other structural configurations of steel SMFs with deep columns must be explored in future investigations. Furthermore, particular attention must be paid to global and local slenderness ratios as well as axial load levels to guarantee ductile behavior of deep columns.

### Declaration of Competing Interest

The authors declare that they have no known competing financial interests or personal relationships that could have appeared to influence the work reported in this paper.

### Acknowledgements

The study presented in this paper is partially supported by two agencies of the government of Mexico: CONACYT and SEP under Grant No. A1-S-10088. Any opinions, findings, conclusions, or recommendations expressed in this article are those of the authors and do not necessarily reflect the views of the Sponsors. In addition, the authors would like to acknowledge the Autonomous University of Sinaloa where some of the authors are affiliated. Finally, the authors would like to thank the unknown Reviewers of the paper.

### References

[1] Aisc. Steel construction manual. Chicago, Illinois 60601–1802: American Institute of Steel Construction; 2017.
[2] AISC 341-16 (2016), *Seismic provisions for structural steel buildings*, American Institute of Steel Construction, Inc., Chicago, IL.
[3] ASCE 7-16 (2017). Minimum Design Loads for Buildings and Other Structures. American Society of Civil Engineers (ASCE), Reston, Virginia 20191.
[4] ATC-24. Guidelines for cyclic seismic testing of components of steel structures. Report prepared for the Applied Technology Council (ATC): Redwood City; 1992.
[5] Boushehri K, Tsavdaridis KD, Cai G. Seismic behaviour of RWS moment connections to deep columns with European sections. J Constr Steel Res 2019;161:416–35. http://dx.doi.org/10.1016/j.jcsr.2019.07.009.
[6] Cao TJ, Shan L, Xiao Y. Numerical studies on full-scale steel columns under complex seismic loading. J Constr Steel Res 2020;172:106227. http://dx.doi.org/10.1016/j.jcsr.2020.106227.
[7] Chi B, Uang CM. Cyclic response and design recommendations of reduced beam section moment connections with deep columns. J Struct Eng 2002;128(4):464–73. http://dx.doi.org/10.1061/(ASCE)0733-9445(2002)128:4(464).
[8] Elkady A, Lignos DG. Analytical investigation of the cyclic behavior and plastic hinge formation in deep wide-flange steel beam-columns. Bull Earthq Eng 2015;13(4):1097–118. http://dx.doi.org/10.1007/s10518-014-9640-y.
[9] Elkady A, Lignos DG. Full-scale testing of deep wide-flange steel columns under multiaxis cyclic loading: loading sequence, boundary effects, and lateral stability bracing force demands. J Struct Eng 2018;144(2):04017189. http://dx.doi.org/10.1061/(ASCE)ST.1943-541X.0001937.
[10] FEMA-350 (2000). *Recommended seismic design criteria for new steel moment-frame buildings*, Federal Emergency Management Agency (FEMA).
[11] FEMA-351 (2000). *Recommended Seismic Evaluation and Upgrade Criteria for Existing Welded Steel Moment-Frame Buildings*, Federal Emergency Management Agency (FEMA).
[12] FEMA-352 (2000). *Recommended Post-earthquake Evaluation and Repair Criteria for Welded Steel Moment-Frame Buildings*, Federal Emergency Management Agency (FEMA).
[13] FEMA-353 (2000). Recommended Specifications and Quality Assurance Guidelines for Steel Moment-Frame Construction for Seismic Applications, Federal Emergency Management Agency (FEMA).
[14] FEMA-354 (2000). *A Policy Guide to Steel Moment Frame Construction*, Federal Emergency Management Agency (FEMA).
[15] FEMA-355C (2000). *State of the art report on systems performance of steel moment frames subject to earthquake ground shaking*, Federal Emergency Management Agency (FEMA).
[16] FEMA-355F (2000). *State of the art report on performance prediction and evaluation of steel moment-frame buildings*, Federal Emergency Management Agency (FEMA).
[17] Fogarty J, Wu TY, El-Tawil S. Collapse response and design of deep steel columns subjected to lateral displacement. J Struct Eng 2017;143(9):04017130. http://dx.doi.org/10.1061/(ASCE)ST.1943-541X.0001848.
[18] Gaxiola-Camacho JR, Azizsoltani H, Villegas-Mercado FJ, Haldar A. A novel reliability technique for implementation of performance-based seismic design of structures. Eng Struct 2017;142:137–47. http://dx.doi.org/10.1016/j.engstruct.2017.03.076.
[19] Gaxiola-Camacho JR, Haldar A, Azizsoltani H, Valenzuela-Beltran F, Reyes-Salazar A. Performance-based seismic design of steel buildings using rigidities of connections. ASCE-ASME Journal of Risk and Uncertainty in Engineering Systems Part A: Civil Engineering 2018;4(1):04017036. http://dx.doi.org/10.1061/AJRUA6.0000943.
[20] Ghobarah A. Performance-based design in earthquake engineering: state of development. Eng Struct 2001;23(8):878–84. http://dx.doi.org/10.1016/S0141-0296(01)00036-0.
[21] Haldar A, Mahadevan S. Probability, reliability, and statistical methods in engineering design. John Wiley & Sons; 2000.
[22] Hamburger RO, Hooper JD. Performance-based seismic design. Modern Steel Construction 2011;51(4):36–9. https://www.aisc.org/globalassets/modern-steel/archives/2011/04/2011v04_performance_based.pdf.
[23] Hamburger, R. O., Krawinkler, H., Malley, J. O., Adan, S. M. (2009). *Seismic design of steel special moment frames: a guide for practicing engineer*, NEHRP Seismic Design Technical Brief No. 2, NIST, Gaithersburg, MD.
[24] Khuri AI, Cornell JA. Response surfaces: designs and analyses. CRC Press; 1996.
[25] Malley, J. , Carter, C. , Hajjar, J. , Lignos, D. , Roeder, C. & Saunders, M. (2011). Research Plan for the Study of Seismic Behavior and Design of Deep, Slender Wide Flange Structural Steel Beam-Column Members. Grant/Contract Reports (NISTGCR). *National Institute of Standards and Technology*, Gaithersburg, MD. 10.6028/nist.gcr.11-917-13.
[26] Mehrabian A, Haldar A, Reyes-Salazar A. Seismic response analysis of steel frames with post-Northridge connection. Steel and Composite Structures 2005;5(4):271–87.
[27] Ozkula G, Uang CM, Harris J. Development of enhanced seismic compactness requirements for webs in wide-flange steel columns. J Struct Eng 2021;147(7):04021100. http://dx.doi.org/10.1061/(ASCE)ST.1943-541X.0003036.
[28] Reyes-Salazar A. Ductility demands of low-, mid-and high-rise steel buildings with medium and deep columns. Earthquakes and Structures 2021;20(6):583–98. https://doi.org/10.12989/eas.2021.20.6.583.
[29] Reyes-Salazar A, Haldar A. Nonlinear seismic response of steel structures with semi-rigid and composite connections. J Constr Steel Res 1999;51(1):37–59. http://dx.doi.org/10.1016/S0143-974X(99)00005-X.
[30] Reyes-Salazar A, Soto-Lopez ME, Gaxiola-Camacho JR, Bojorquez E, Lopez-Barraza A. Seismic response estimation of steel buildings with deep columns and PMRF. Steel and Composite Structures 2014;17(4):471–95. https://doi.org/10.12989/scs.2014.17.4.471.

[31] Richard RM, Allen CJ, Partridge JE. Proprietary slotted beam connection designs. Modern Steel Construction 1997:28–33. https://www.aisc.org/globalassets/modern-steel/archives/1997/03/1997v03_proprietary_designs.pdf.

[32] Sabol TA. An assessment of seismic design practice of steel structures in the United States since the Northridge earthquake. The Structural Design of Tall and Special Buildings 2004;13(5):409–23. http://dx.doi.org/10.1002/tal.282.

[33] Shen JHJ, Astaneh-Asl A, McCallen DB. Use of deep columns in special steel moment frames. Steel Tip Rep 2002;24. https://citeseerx.ist.psu.edu/viewdoc/download?doi=10.1.1.535.8392&rep=rep1&type=pdf.

[34] Somerville, P.G. (1997). Development of ground motion time histories for phase 2 of the FEMA/SAC steel project: SAC Joint Venture. https://store.atcouncil.org/index.php?dispatch=products.view&product_id=152.

[35] Sophianopoulos DS, Deri AE. Parameters affecting response and design of steel moment frame reduced beam section connections: an overview. International Journal of Steel Structures 2011;11(2):133–44. http://dx.doi.org/10.1007/s13296-011-2003-5.

[36] Wu TY, El-Tawil S, McCormick J. Highly ductile limits for deep steel columns. J Struct Eng 2018;144(4):04018016. http://dx.doi.org/10.1061/(ASCE)ST.1943-541X.0002002.

[37] Wu TY, El-Tawil S, McCormick J. Seismic collapse response of steel moment frames with deep columns. J Struct Eng 2018;144(9):04018145. http://dx.doi.org/10.1061/(ASCE)ST.1943-541X.0002150.

[38] Zhang X, Ricles JM. Experimental evaluation of reduced beam section connections to deep columns. J Struct Eng 2006;132(3):346–57. http://dx.doi.org/10.1061/(ASCE)0733-9445(2006)132:3(346).